Chem

CellPress

Article

Merging Photoredox PCET with Ni-Catalyzed Cross-Coupling: Cascade Amidoarylation of Unactivated Olefins

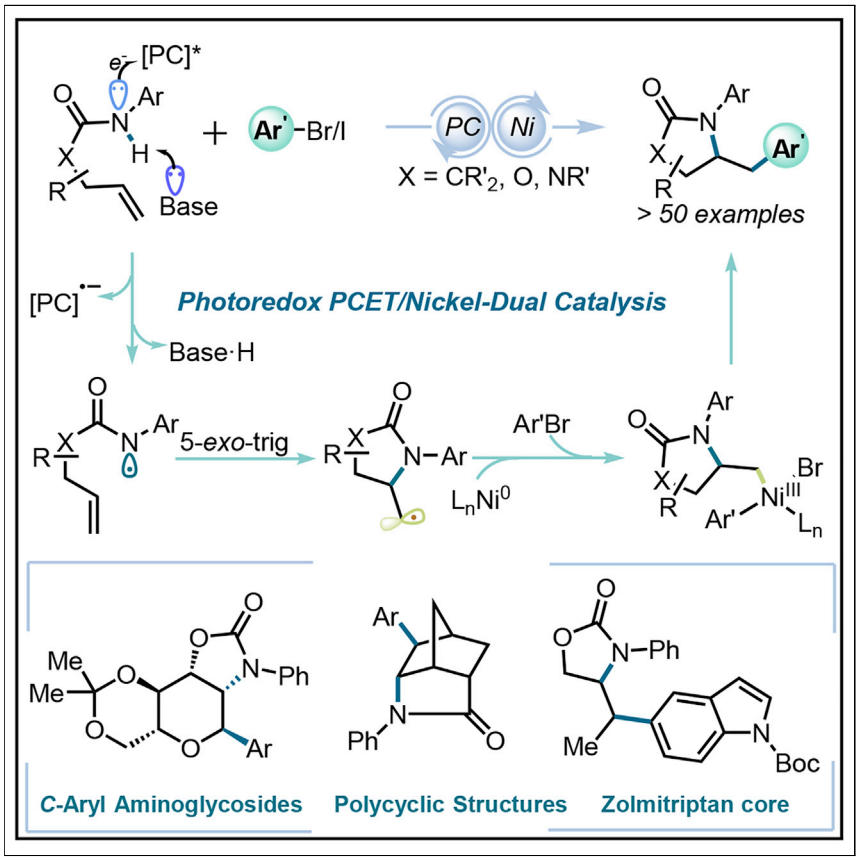

A rapid, highly diastereoselective amidoarylation of unactivated olefins was achieved to render medicinally privileged pyrrolidinone structures. Taking advantage of a photoredox proton-coupled electron transfer process, amidyl radicals were obtained from non-prefunctionalized N–H bonds under mild conditions, which were subsequently trapped by pendant olefins, delivering alkyl radicals for nickel-catalyzed cross-coupling. Mechanistic studies revealed the key balance between thermodynamically-driven radical generation and kinetically-driven cyclization, which led to expanding the scope toward urea and carbamate substrates.

Shuai Zheng, Álvaro Gutiérrez-Bonet, Gary A. Molander

gmolandr@sas.upenn.edu

HIGHLIGHTS

Generation of C-centered radicals via cleavage of strong X–H bonds for cross-coupling

Rapid formation of new N–C_{sp3} and C_{sp2}–C_{sp3} bonds from olefins under mild conditions

Highly diastereoselective synthesis of medicinally privileged pyrrolidinone structures

Mechanism-driven scope expansion toward carbamate and urea motifs

Zheng et al., Chem 5, 1–14
February 14, 2019
https://doi.org/10.1016/j.chempr.2018.11.014

Please cite this article in press as: Zheng et al., Merging Photoredox PCET with Ni-Catalyzed Cross-Coupling: Cascade Amidoarylation of Unactivated Olefins, Chem (2018), https://doi.org/10.1016/j.chempr.2018.11.014

Chem

CellPress

Article

Merging Photoredox PCET with Ni-Catalyzed Cross-Coupling: Cascade Amidoarylation of Unactivated Olefins

Shuai Zheng,[1,2] Álvaro Gutiérrez-Bonet,[1,2] and Gary A. Molander[1,3,*]

SUMMARY

The integration of amidyl radicals with cross-coupling chemistry opens new avenues for reaction design. However, the lack of efficient methods for the generation of such radical species has prevented many such transformations from being brought to fruition. Herein, the amidoarylation of unactivated olefins by a cascade process from non-functionalized amides is reported by merging, for the first time, photoredox proton-coupled electron transfer (PCET) with nickel catalysis. This new technology grants access to an array of complex molecules containing a privileged pyrrolidinone core from alkenyl amides and aryl- and heteroaryl halides in the presence of a visible light photocatalyst and a nickel catalyst. Notably, the reaction is not restricted to amides—carbamates and ureas can also be used. Mechanistic studies, including hydrogen-bond affinity constants, cyclization rate measurements, quenching studies, and cyclic voltammetry, were central to comprehend the subtleties contributing to the integration of the two catalytic cycles.

INTRODUCTION

The recent disclosure of nickel/photoredox dual catalysis has made cross-coupling chemistry an even more important tool for synthetic chemists.[1–7] Under mild conditions with excellent functional group tolerance, these powerful methods have facilitated the construction of numerous challenging C_{sp2}–C_{sp3}[1–7] and C_{sp3}–C_{sp3}[8] bonds, transformations that are crucial for success in modern drug discovery.[9] Although powerful and enabling, most of the radical precursors contain a traceless redox handle previously introduced via multi-step synthesis[1,2,6,7] that is homolytically cleaved, generating the desired radical species. Ideally, if radicals were generated from native functional groups benefiting from innate reactivity, excellent atom- and step-efficiencies could be achieved on top of the many other existing advantages associated with Ni/photoredox dual catalysis (e.g., mild reaction conditions, good chemoselectivity, and reduced risks of side reactions).

In this vein, significant achievements have been reached by merging hydrogen atom transfer (HAT) of activated C–H bonds with Ni-catalyzed cross-coupling reactions.[4,5] However, there has been a lack of reports in which heteroatom-centered radicals, derived from the homolytic cleavage of heteroatom–hydrogen bonds, are used as initial intermediates in a sequence of transformations, leading to subsequent C_{sp2}–C_{sp3} bond construction.[10] In fact, if the generation of such radicals could be coupled with a cyclization onto naturally abundant olefins, one could not only maintain excellent atom economy while accessing privileged heterocyclic scaffolds, but also transform relatively unreactive olefins to reactive, nucleophilic *C*-centered

The Bigger Picture

Rapid generation of molecular complexity and access to novel 3D chemical space is pivotal for successful and efficient drug discovery. Nickel/photoredox dual catalysis has arisen as an appealing strategy toward such a goal by rapidly introducing C_{sp3} centers under mild reaction conditions. By taking advantage of a native amide group, we achieved an amidoarylation reaction of unactivated olefins, rendering a series of medicinally privileged structures in a highly atom-economical way. The reaction takes advantage of a photoredox proton-coupled electron transfer event to cleave the strong amidyl N–H bond homolytically. Subsequent regiospecific 5-*exo*-*trig* cyclization generates an alkyl radical. High functional group tolerance was achieved with excellent diastereoselectivities owing to the reaction's mild nature. Mechanistic studies showed the intricate relationship between the base stoichiometry and the N–H donor, as well as the key balance between kinetic and thermodynamic factors.

Please cite this article in press as: Zheng et al., Merging Photoredox PCET with Ni-Catalyzed Cross-Coupling: Cascade Amidoarylation of Unactivated Olefins, Chem (2018), https://doi.org/10.1016/j.chempr.2018.11.014

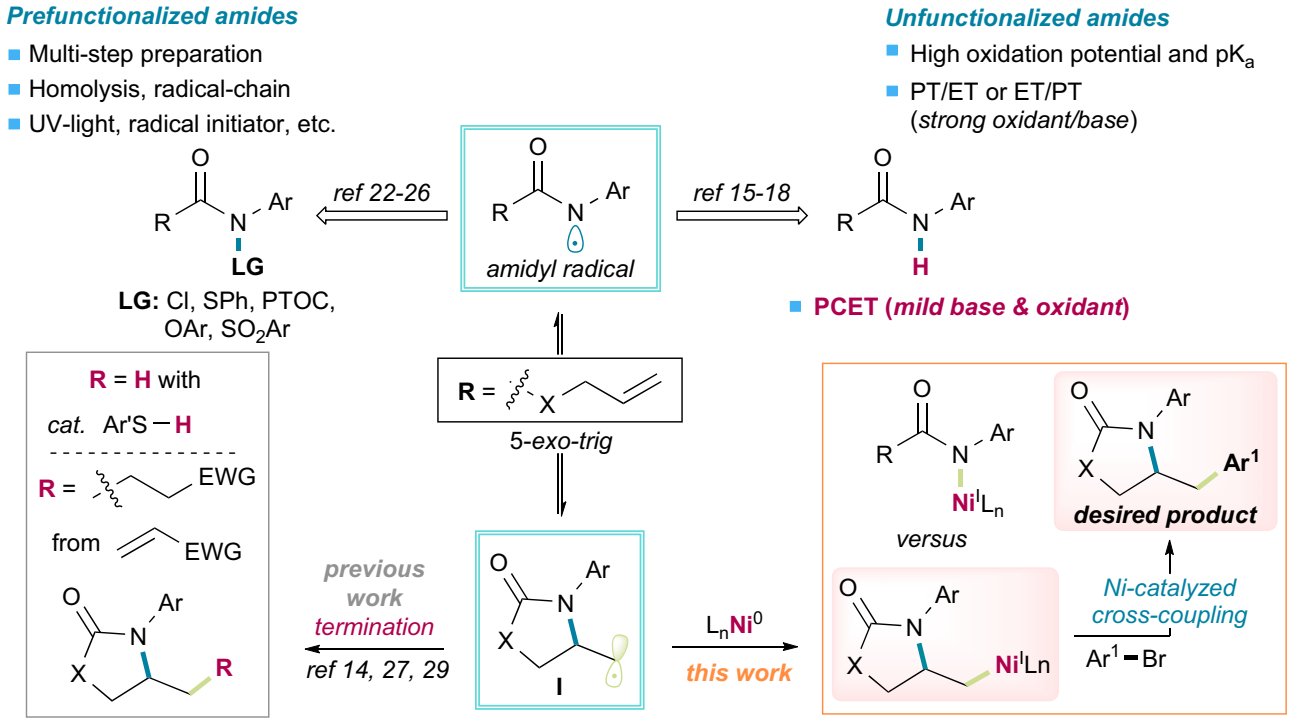

Scheme 1. Generation of Amidyl Radicals from Functionalized and Non-functionalized Amides

radicals, thereby providing new opportunities for rapidly increasing molecular complexity via novel radical cyclization/cross-coupling paradigms.

Owing to the prevalence of nitrogen-containing heterocycles in Food and Drug Administration-approved small-molecule drugs,[11] an investigation was undertaken to explore the applicability of amidyl radicals, generated via homolytic N–H cleavage, to synthesize nitrogen-containing heterocycles via a radical cyclization/cross-coupling paradigm. The generation of amidyl radicals from N–H bonds has previously posed significant challenges because of their high stability (bond-dissociation free energy ~100 kcal/mol).[12–18] As a result, amidyl radical formation was only achieved using strong oxidants (e.g., Dess-Martin periodinane,[15] iodoxybenzoic acid,[16] di-*tert*-butyl peroxide[17]) at high temperatures (Scheme 1),[15–18] seriously compromising the applicability of the developed methods. Alternatively, the use of prefunctionalized amides[19–21] (e.g., LG = Cl,[22] SPh,[23] PTOC [pyridine-2-thione-*N*-oxycarbonyl],[24] OAr,[25] or SO_2Ar[26]) made amidyl radicals more accessible under various conditions (i.e., UV light, radical initiators, reductants). However, this approach posed numerous disadvantages, such as the requirement for multi-step syntheses of the amide derivatives, poor stability of the functionalized amides, and the use of hazardous reagents, among others.

In a seminal publication, the Knowles group reported the generation of amidyl radicals by merging concerted proton-coupled electron transfer (PCET) with photoredox catalysis (Scheme 1).[14,27–29] After adoption of the biologically ubiquitous PCET mechanism,[30,31] this challenging bond disconnection was realized under very mild conditions by emphasizing a much lower-barrier concerted pathway, where charged intermediates are avoided.[15–17] Mechanistic studies showed that upon hydrogen bonding with a phosphate base, the amidyl radical was generated

[1]Roy and Diana Vagelos Laboratories, Department of Chemistry, University of Pennsylvania, 231 South 34th Street, Philadelphia, PA 19104-6323, USA

[2]These authors contributed equally

[3]Lead Contact

*Correspondence: gmolandr@sas.upenn.edu

https://doi.org/10.1016/j.chempr.2018.11.014

Please cite this article in press as: Zheng et al., Merging Photoredox PCET with Ni-Catalyzed Cross-Coupling: Cascade Amidoarylation of Unactivated Olefins, Chem (2018), https://doi.org/10.1016/j.chempr.2018.11.014

via single-electron transfer oxidation by the excited photocatalyst. Subsequent addition of the amidyl radical across the pendant alkene resulted in a *C*-centered radical, which was quenched via hydrogen atom abstraction or Giese-type addition to a Michael acceptor.[14,27,32]

Being aware of the potential of alkene difunctionalization strategies for the rapid construction of molecular complexity,[15,33–36] a means was sought to use PCET to expand the repertoire of current organic synthetic transformations in this realm. Indeed, this scenario to some extent mimics some stages of the dual catalysis that we have been conducting with different radical precursors, whereby alkyl radicals generated via reductive quenching of photocatalysts were merged with a nickel-catalyzed cross-coupling cycle with different aryl electrophiles.[1,2] Based on our previous experience, a process was envisioned that would benefit from the rapid 5-*exo*-trig cyclization of amidyl radicals ($k \sim 10^5\ s^{-1}$)[37] generated via PCET to funnel the resulting alkyl radical into a nickel-catalyzed cross-coupling cycle, resulting in the introduction of biologically relevant pyrrolidinone cores[11] onto aromatic backbones.

This novel photoredox PCET/Ni dual catalytic strategy would be expected to expedite the synthesis of medicinally privileged *N*-containing heterocyclic scaffolds. Importantly, there are several notable examples of bioactive molecules with this structure, such as zolmitriptan and cytochalasin B (Figure 1). It is also worth noting that, whereas other aminoarylation strategies rely on harsh reaction conditions[38,39] or very reactive arylating reagents,[40,41] this new strategy would benefit from the mild reaction conditions associated with photoredox catalysis and PCET mechanisms, providing ample opportunities for the high chemoselectivity profile required for the late-stage construction of densely functionalized molecules. Moreover, the proposed transformation would not necessarily be restricted to amides, so that carbamates and ureas could also be employed, expanding the array of heterocyclic cores within range. Carbamates are particularly interesting, considering the tremendous number of bioactive molecules containing allylic alcohols (Figure 1) that might be engaged in this transformation through conversion to the carbamate, as well as the ease of carbamate motif installation via quantitative alcoholysis of aryl isocyanates. Notably, thanks to the ease of oxazolidinone hydrolysis, ring-opened derivatives would be readily accessible,[16,42] resulting in a formal three-component difunctionalization of unactivated olefins (Figure 1). Together with other derivatization possibilities such as reduction,[42,43] a series of cyclic or acyclicamido- or aminoarylated backbones could be constructed.

RESULTS AND DISCUSSION

Reaction Discovery and Optimization

Prior to the search for suitable reaction conditions, an analysis was undertaken of the possible challenges in developing this demanding, yet appealing, transformation. Although 5-*exo*-*trig* cyclization was expected to be fast, a low thermodynamic driving force ($\Delta G^\circ \approx -3$ to -5 kcal/mol in the transformation of amidyl to 1° or 2° alkyl radicals) was anticipated to be non-optimal for the reaction progress.[12,44] Indeed, in a previous hydroamination study, a thiophenol HAT catalyst was required to drive the transformation to completion.[27] Moreover, the coexistence of amidyl and alkyl radical species in the reaction medium could lead to selectivity issues, depending on the affinity of the nickel complexes for these species and the energy barrier of the subsequent step. This provided the potential for the generation of mixtures of *N*-arylated and olefin amidoarylated products.[17] With these challenges in mind, an investigation was begun using pent-4-enylanilide **S1** and

Please cite this article in press as: Zheng et al., Merging Photoredox PCET with Ni-Catalyzed Cross-Coupling: Cascade Amidoarylation of Unactivated Olefins, Chem (2018), https://doi.org/10.1016/j.chempr.2018.11.014

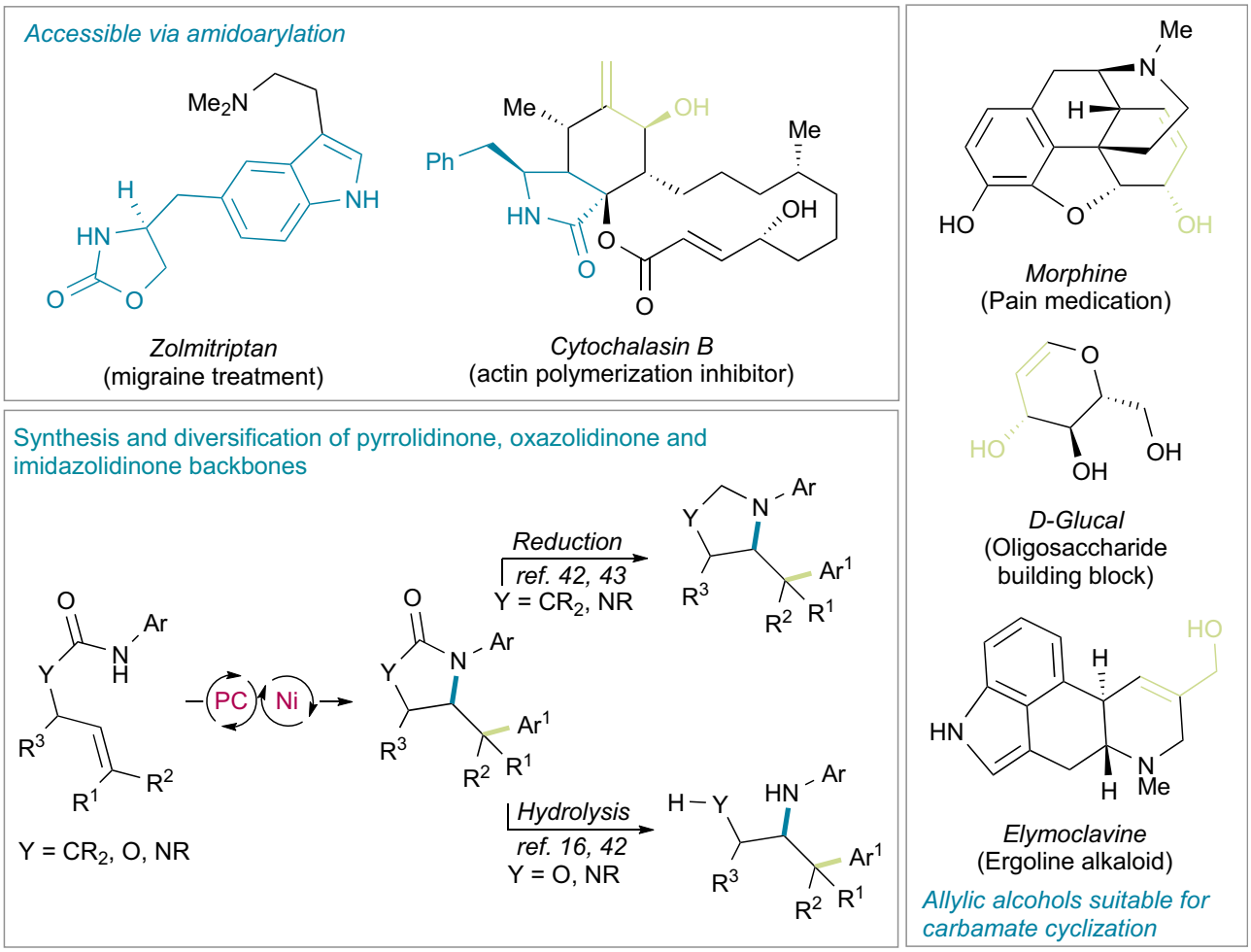

Figure 1. Biological Relevance, Diversification of "Lidinone" Derivatives, and Naturally Occurring Allylic Alcohols

4-bromobenzonitrile as reaction partners. Initial screening using a mildly oxidizing Ir-photocatalyst (**Ir-1**) ($E_{1/2}$* = 1.32 V versus standard carbon electrode [SCE]) and the weak base $Bu_4N[OP(O)(OBu)_2]$ (pK_a = 1.72)[45] led to a 29% yield of the expected product **1** (Figure 2, entry 1). Ir-based photocatalysts with higher oxidizing power (entries 2 and 3) gave lower yields or no product at all, likely owing to a poorer rate match between the two catalytic cycles or relative instability of the photocatalyst. Stronger bases favoring the formation of the corresponding amidate, such as KO*t*-Bu (entry 4), proved unsuccessful in this case. However, higher amounts of the phosphate base translated into higher yields (entry 6). The necessity for superstoichiometric amounts of $Bu_4N[OP(O)(OBu)_2]$ was further validated after seeing failures at attempting to use it catalytically in combination with inorganic bases to regenerate the former over the course of reaction (entry 5). Supporting the initial mechanistic hypothesis, these conditions, along with the physical properties of the anilide (pK_a of ~21[13] and redox potential of 1.78 V [versus SCE]), suggest that the cleavage of the anilide N–H bond is most likely occurring via a concerted PCET pathway. Both Ni(II) and Ni(0) sources rendered similar yields (entries 6 and 9). Consequently, well-defined Ni(dMeObpy)$(H_2O)_2Br_2$ was used as the catalyst precursor based on its stability, ease of preparation, and more convenient reaction setup. Among the several bipyridyl-type ligands tested, dMeObpy clearly stood

Please cite this article in press as: Zheng et al., Merging Photoredox PCET with Ni-Catalyzed Cross-Coupling: Cascade Amidoarylation of Unactivated Olefins, Chem (2018), https://doi.org/10.1016/j.chempr.2018.11.014

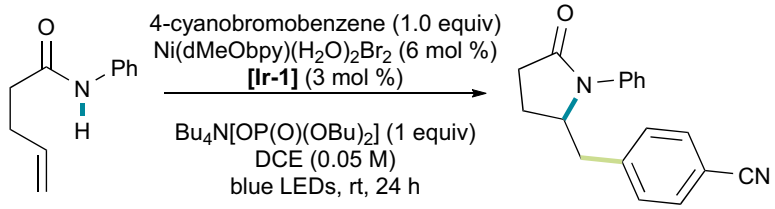

S1 **1**

entry	variation from standard conditions[a]	yield (%)[b]
1	none	29
2	**[Ir-2]** instead of **[Ir-1]**	25
3	**[Ir-3]** instead of **[Ir-1]**	0
4	*t*-BuOK instead of $Bu_4N[OP(O)(OBu)_2]$	0
5	2.5 equiv Cs_2CO_3 + 10 mol % $Bu_4N[OP(O)(OBu)_2]$	< 5
6	$Bu_4N[OP(O)(OBu)_2]$ (2.5 equiv)	51

entry	variation from entry 6[a]	yield (%)[b]
7	$Ni(phen)Br_2$ instead of $Ni(dMeObpy)Br_2$	45
8	$Ni(dtbbpy)Br_2$ instead of $Ni(dMeObpy)Br_2$	42
9	$Ni(COD)_2$ + dMeObpy	50
10	*t*-BuOH instead of DCE	68
11	***t*-BuOH/PhCF$_3$ (2:1)**	**78**

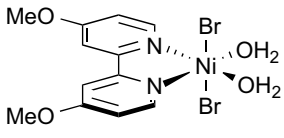

$Ni(dMeObpy)(H_2O)_2Br_2$

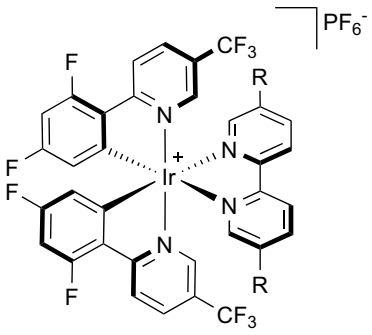

Ir-photocatalyst

[Ir-1]; R = H; E_{PC^*/PC^-} = 1.32 V (SCE)

[Ir-2]; R = F; E_{PC^*/PC^-} = 1.61 V (SCE)

[Ir-3]; R = CF_3; E_{PC^*/PC^-} = 1.68 V (SCE)

Figure 2. Optimization of Reaction Conditions

[a]Reactions were performed on a 0.3-mmol scale. [b]Yield of isolated product after column chromatography.

out, likely owing to easier oxidative addition with aryl halides because of its more electron-rich nature.

Attempting to increase the reaction yield, we investigated the by-products generated over the course of the reaction. Among the few identified, chlorobenzonitrile was, by far, predominant. We reasoned that the 1,2-dichloroethane (DCE) was responsible for the formation of this by-product, being the only chloride source present in the reaction medium.[46] After confirming that aryl chlorides are inert under reaction conditions, we examined other non-chlorinated solvents to avoid the consumption of the aryl bromide and its deleterious effect on yield. Upon testing numerous options, *t*-BuOH proved to be an excellent replacement, affording considerably enhanced yields (entry 10). We suggest that this improvement is likely due to an acidity enhancement of the N-H bond by the *t*-BuOH. Finally, in an attempt to match DCE's polarity, different binary solvent systems with *t*-BuOH were tested. In the event, a 78% yield was obtained using a 2:1 *t*-BuOH/$PhCF_3$ mixture (entry 11), which came as no surprise considering the beneficial effects of α,α,α-trifluorotoluene in radical reactions.[32] As expected, control experiments showed the key role played by all of the reaction components.[47]

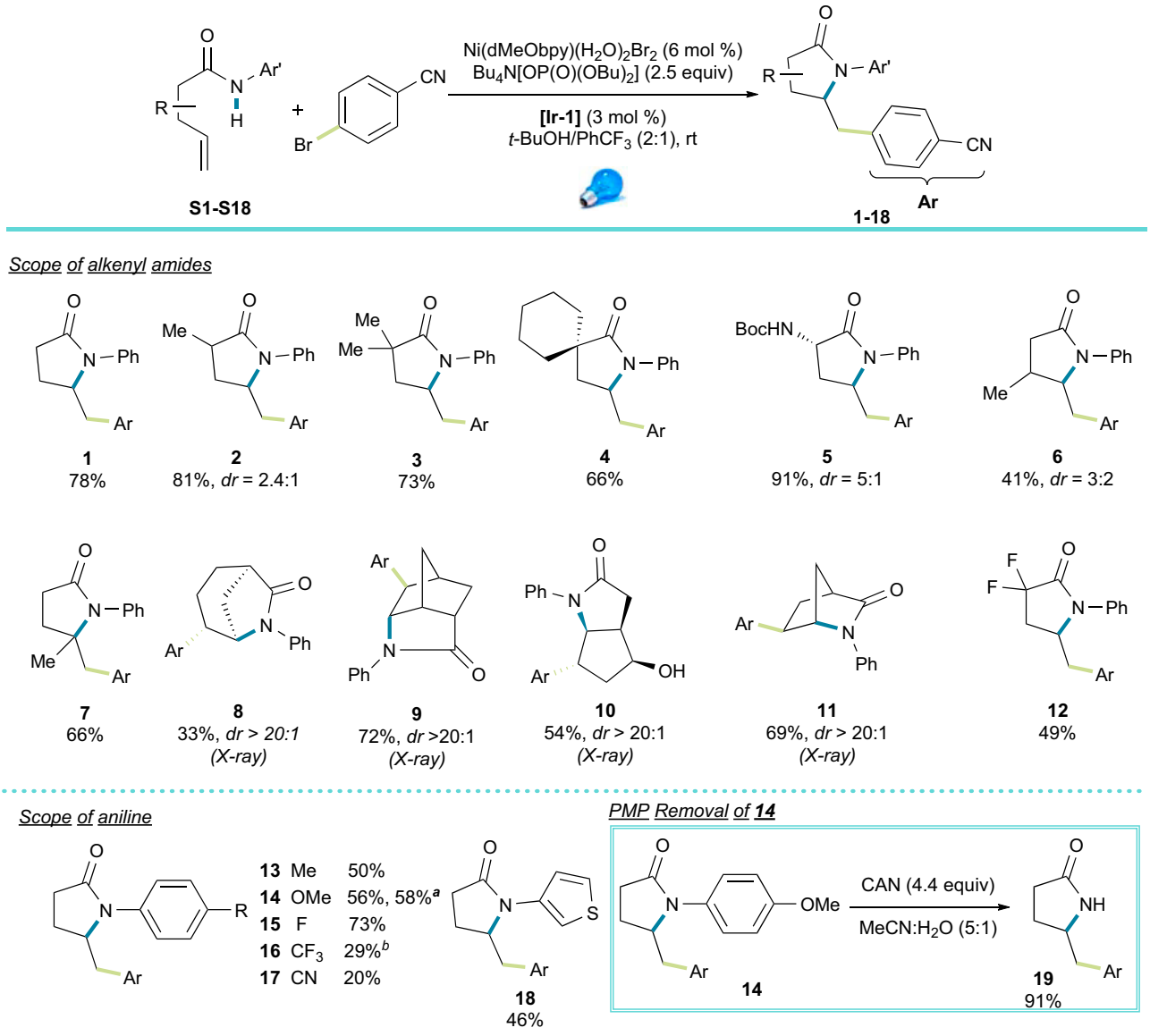

Figure 3. Scope of *N*-Arylated Alkenyl Amides

Reaction conditions: amide **S1–S18** (0.36 mmol, 1.2 equiv), 4-bromobenzonitrile (0.3 mmol, 1.0 equiv), $Bu_4N[OP(O)(OBu)_2]$ (0.75 mmol, 2.5 equiv), Ni(dMeObpy)$(H_2O)_2Br_2$ (0.018 mmol, 6 mol %), [**Ir-1**] (0.009 mmol, 3 mol %), blue LED, 6 mL *t*-BuOH/$PhCF_3$ (2:1). [a] Reaction run on 5 mmol scale. [b] [**Ir-2**] was used.

Substrate Scope Studies

Subsequently, the limits of this reaction were explored via substrate scope study. As shown in Figure 3, substitutions from the α to the γ positions on the amide are all accommodated, allowing the synthesis of a tetra-substituted carbon center (**7**). Notably, no significant Thorpe-Ingold effect was observed when comparing differently α-substituted substrates (**1–3**). A series of bicyclic (**8**, **10**, **11**), tricyclic (**9**), and spirocyclic structures (**4**) were accessible from simple precursors. Remarkably, when an endocyclic double bond was involved, the reaction in all cases showed diastereoselectivities greater than 20:1 in favor of the *trans* product (**8–11**). Protic functional groups such as hydroxy (**10**) and carbamate (**5**) did not pose a problem, nor did activated α protons. Excellent regioselectivity was achieved, with no 6-*endo*-trig cyclization observed in any of the substrates examined. A notable yield drop was

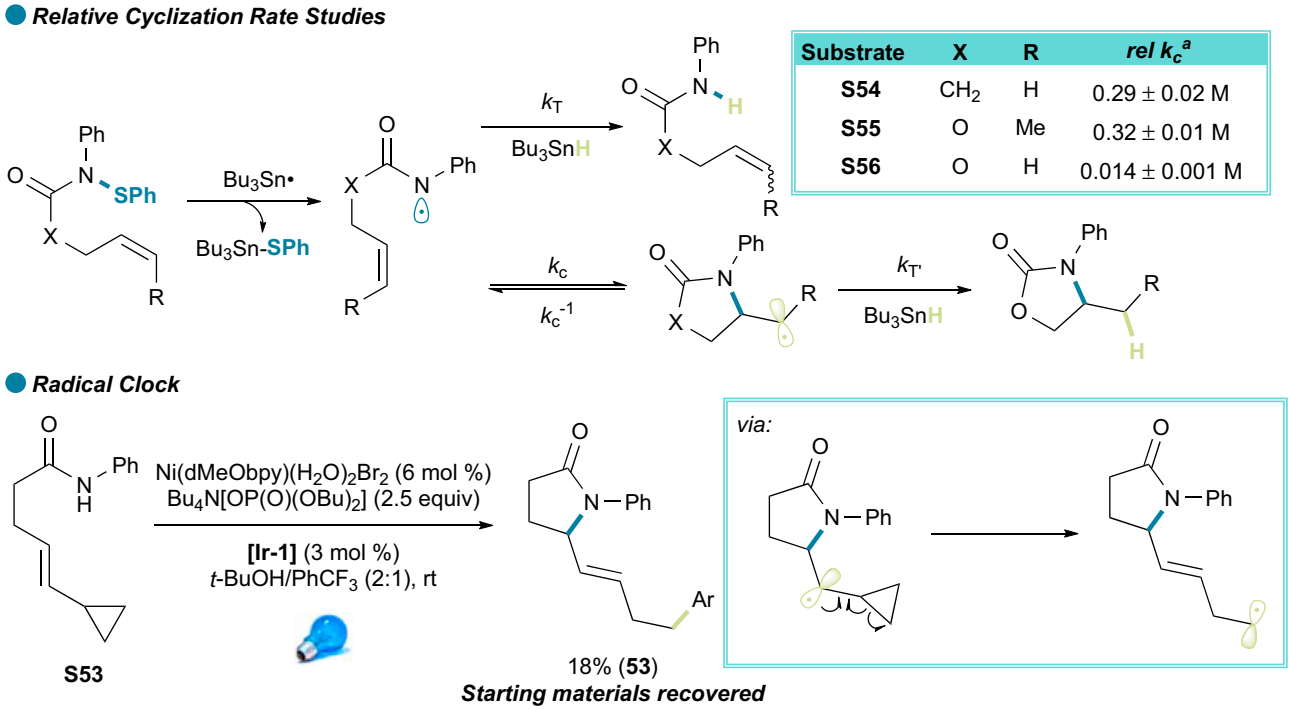

Scheme 2. Relative Cyclization Rate Studies and Radical Clock Experiment

[a]The values reported are relative to k_T. See Figure S1 for further details.

observed using an α,α-difluorosubstituted amide (**12**), most likely because of the higher oxidation potential of this more electron-deficient amide (2.03 V versus 1.78 V for non-substituted pentenamide **S1**). In line with this observation, when a more electron-deficient anilide was involved, a significantly lower yield was observed (**16**, **17**). The more oxidizing photocatalyst [**Ir-2**] had to be applied to form **16**, because [**Ir-1**] failed to give any product. We reasoned that the former favored the amidyl radical formation, whereas the latter was not oxidizing enough to accomplish the formation of that intermediate. Electron-neutral and electron-rich anilines or heteroaryl amines (**13**–**15**, **18**) delivered the corresponding products in moderate to good yields. Considering that *N*-aryl amides are required to facilitate the PCET step, *para*-methoxyphenyl (PMP) was incorporated as the aryl motif, which allowed the synthesis of unsubstituted pyrrolidinones upon removal of the PMP group with ceric ammonium nitrate (**19**).[48] Moreover, a gram-scale reaction was carried out without further optimization on the PMP-protected substrate (**14**) with no erosion in the yield, thus establishing the scalability of this reaction.

Excellent functional group tolerance was observed when different aryl bromides were subjected to the reaction conditions, including electron-deficient and electron-neutral substrates (**20**, **22**–**35**, **37**), featuring functional units such as aldehydes, boronates, sulfones, amides, esters, trifluoromethoxy groups, and various halides. Electron-rich aryl bromides were challenging, probably because of the more demanding oxidative addition step, yet good yields could be achieved using the corresponding aryl iodides (**21**, **36**, and **49**). Similarly, because of the more challenging oxidative addition, relatively electron-neutral (hetero)aryl bromides (e.g., **23**, **32**, and **39**) and *ortho*-substituted aryl bromides (**33**) exhibited diminished efficiency, with the remaining anilide starting material and (hetero)aryl bromides recovered after purification. Notably, aryl iodides only seemed to work on electron-rich

Please cite this article in press as: Zheng et al., Merging Photoredox PCET with Ni-Catalyzed Cross-Coupling: Cascade Amidoarylation of Unactivated Olefins, Chem (2018), https://doi.org/10.1016/j.chempr.2018.11.014

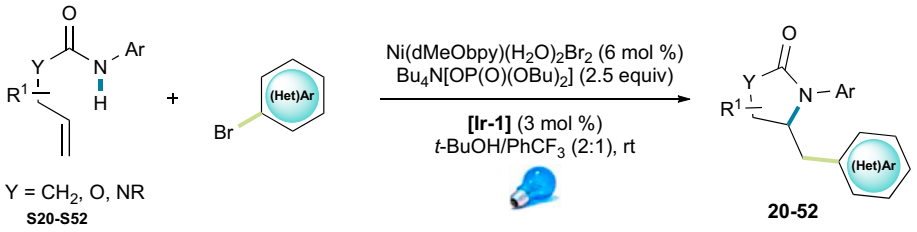

Scope of aryl halides

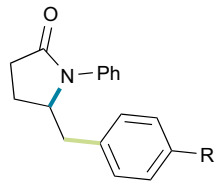

20	R = acetyl	68%
21	OMe	51%[a]
22	OCF_3	75%
23	Ph	31%
24	$CONMe_2$	72%
25	Br	55%
26	B(Neop)	55%
27	CO_2Me	57%
28	SO_2Me	72%
29	CHO	63%

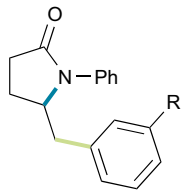

30	R = OMe	78%
31	Me	47%
32	F	36%

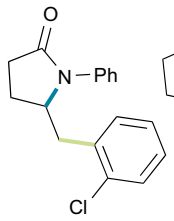

33
36%

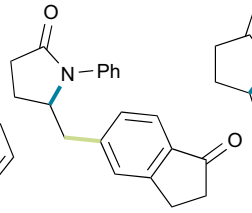

34
67%

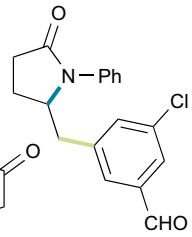

35
64%

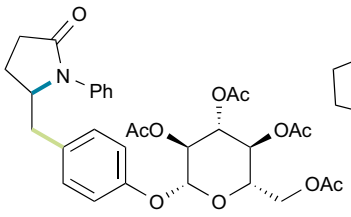

36
58%,[a] *dr* = 1:1

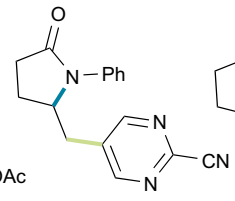

37
72%

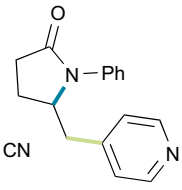

38
80%

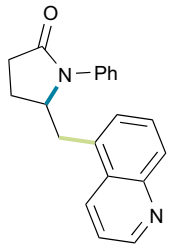

39
40%

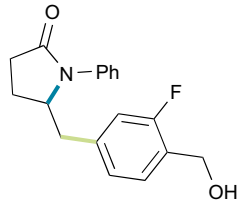

40
61%

Scope of carbamates and ureas

Ar = 4-benzonitrile

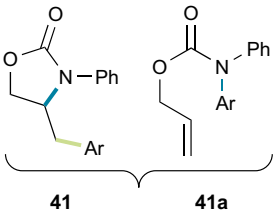

41
22%

41a
37%

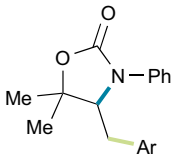

42
32%

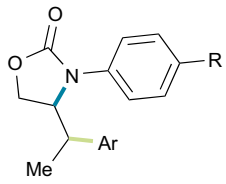

43	R = H	64%(78%[b])
44	acetyl	56%
45	OMe	38%
46	Br	59%
47	CN	38%

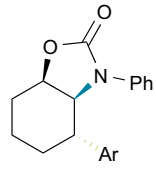

48
51%, *dr* > 20:1
(X-ray)

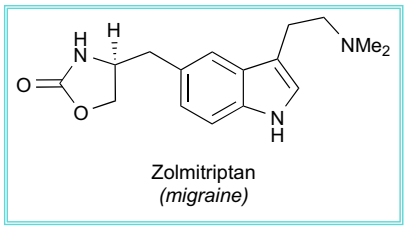

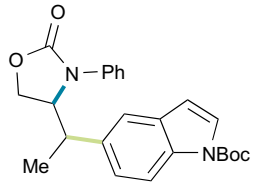

49
55%[a]

Zolmitriptan core

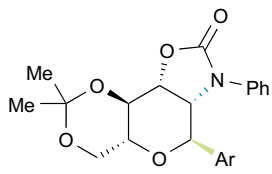

50
83%, *dr* > 20:1

Novel Approach toward *C*-Aryl-Amino Glycosides

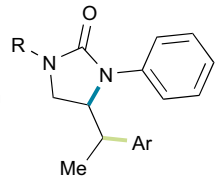

51	R = *n*-Bu	58%
52	Me	53%

Figure 4. Scope of (Hetero)Aryl Halides, Carbamates, and Ureas

Reaction conditions: amide, urea, or carbamate **S20–S52** (0.36 mmol, 1.2 equiv), (hetero)aryl halide (0.3 mmol, 1.0 equiv), $Bu_4N[OP(O)(OBu)_2]$ (0.75 mmol, 2.5 equiv), Ni(dMeObpy)$(H_2O)_2Br_2$ (0.018 mmol, 6 mol %), [**Ir-1**] (0.009 mmol, 3 mol %), blue LED, 6 mL *t*-BuOH/$PhCF_3$ (2:1). [a] (Hetero)aryl iodide was applied. [b] 7.5 equiv of base were used.

systems, whereas electron-neutral or electron-poor substrates rendered compromised yields. Substructures with reducible functional groups or activated hydrogens such as benzylic alcohols (**40**), saccharides (**36**), and aldehydes (**29**, **35**) remained intact under the reaction conditions, demonstrating the highly chemoselective nature of this sequential transformation. In an effort to focus on more medicinally relevant scaffolds, several electron-deficient (**37–39**) or electron-rich (**49**) heteroaryl halides were tested, resulting in modest to high yields of the desired products.

To broaden the utility of this transformation, we tested β,γ-unsaturated aryl carbamates and ureas in an attempt to provide an easy route toward oxazolidinone and imidazolidinone scaffolds. Unfortunately, initial attempts with an *O*-allyl aryl carbamate produced a mixture of *N*-arylation (**41a**) and amidoarylation (**41**) products (37% and 22% yield, respectively).[47] To improve the reaction performance, an all-substituted carbon was placed at the β-position (**42**) to favor the cyclization rate by invoking the Thorpe-Ingold effect. In line with previous observations (**1–3**), the yield enhancement was poor. However, *N*-arylated product was suppressed in this case. Indeed, although a highly reversible amidyl radical addition to nickel has been described,[17] such transformations for carbamate-*N* radicals appear to be unknown.

As a more electron-rich motif compared with amides, nitrogen-based radicals derived from carbamates would be expected to exhibit a higher nucleophilicity, therefore favoring bonding with nickel. To minimize this putative reactivity, we sought a designed motif to enhance the rate of 5-*exo*-*trig* cyclization. Considering that the carbamate's N–H bond-dissociation enthalpy (BDE) (~95 kcal/mol)[13] is lower than that of amides (~100 kcal/mol),[12,14] it becomes evident that, from a thermodynamic standpoint, generation of a primary alkyl radical via cyclization (BDE of primary C–H ~98 kcal/mol)[44] is less favored for carbamates than for amides ($\Delta G^\circ \approx 3$ kcal/mol versus −2 kcal/mol). Owing to the BDE difference between primary and secondary C–H bonds (~4 kcal/mol lower for secondary C–H),[44] we anticipated that internal alkenes would react more smoothly. To test this hypothesis, we carried out an indirect kinetic study using *N*-(phenylthiol)amides as the amidyl radical precursors to determine the relative rate of radical cyclization (Scheme 2 and Figure S1).[23,37] As shown, the cyclization rate for *O*-crotyl phenylcarbamate (**S55**) was ~25 times faster than for *O*-allyl phenylcarbamate (**S56**), thus supporting the notion that generation of a secondary alkyl radical leads to a more efficient cyclization step. Indeed, for both ureas and carbamates, satisfactory yields were obtained when internal alkenes were used (**43–52**, Figure 4). Along this line, amino aryl glycoside **50** derived from galactal was obtained in an 83% yield and excellent diastereoselectivity, suggesting a more efficient cyclization step that can most likely be attributed to stabilization of the generated α-oxy radical. The success of incorporating *N*-Boc-indole (**49**) provides an excellent starting point for the synthesis of zolmitriptan analogs in a straightforward manner, thus highlighting a direct application of this method. Interestingly, for the urea **52**, one of the double bonds remained unreacted without any observable intermolecular transformations.

Mechanistic Insights

Although preliminary results pointed toward a mechanistic pathway in line with our initial proposal (Scheme 1 and Figure 2), further experiments were conducted to

Please cite this article in press as: Zheng et al., Merging Photoredox PCET with Ni-Catalyzed Cross-Coupling: Cascade Amidoarylation of Unactivated Olefins, Chem (2018), https://doi.org/10.1016/j.chempr.2018.11.014

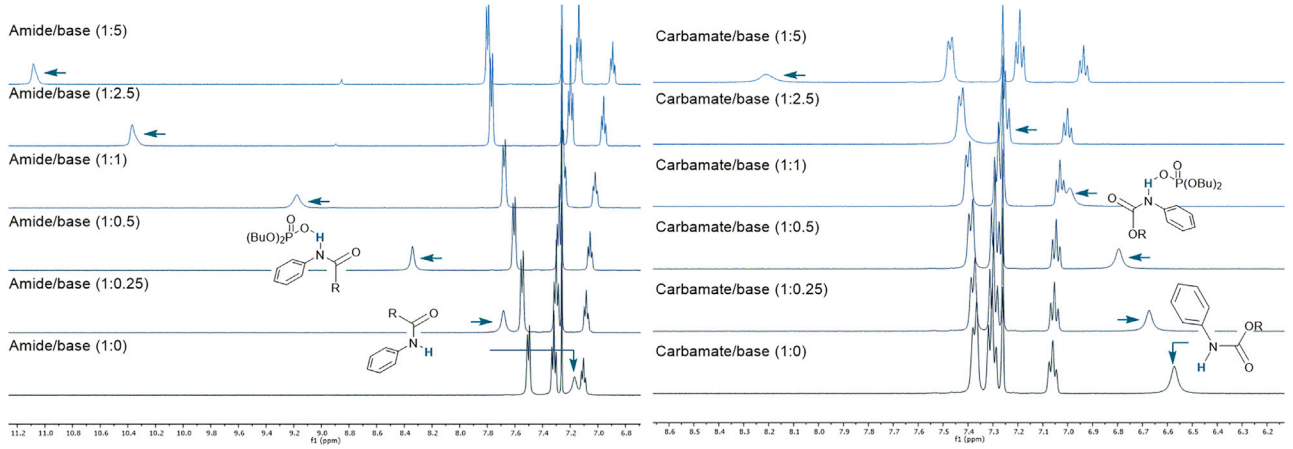

Figure 5. Measuring the Hydrogen-Bonding Affinity of Amides and Carbamates
See also Figures S12–S15 for further details.

substantiate the mechanism. As anticipated, control experiments excluding photocatalyst, nickel precatalyst, base, and light, gave no product (see Table S1).[47] A radical clock experiment (Scheme 2; see also Supplemental Information 4.2) led exclusively to rearranged product **53**, indicating the unlikelihood of undergoing an energy transfer-mediated migratory insertion mechanism or alkene aminometalation.[35] Still, the crucial role for 2.5 equiv of $Bu_4N[OP(O)(OBu)_2]$ base remained unclear. Cyclic voltammetry measurements showed that after addition of 2.5 equiv of base, the redox potential of the amide dropped from 1.78 V to 1.27 V (versus SCE), which is within the [**Ir-1**] photocatalyst excited state oxidative range, thus favoring a PCET mechanistic scenario. However, this potential was also achieved with only 1 equiv of base.[47] Stern-Volmer studies were carried out (see Supplemental Information 4.6) with a fixed ratio of 1:2.5 (substrate/base) to mimic the reaction medium. A linear relationship was observed. Although possessing a narrower linear range, the quenching efficiency of the carbamate-base mixture (Stern-Volmer constant [K_{SV}] = 19,000 $\pm$ 2,000 M^{-1}) was higher than that of amide-base (K_{SV} = 8,200 $\pm$ 700 M^{-1}), consistent with the relative ease of oxidation of the carbamate compared with that of an amide (1.73 V versus SCE for allyl phenylcarbamate **S41**, 1.18 V after addition of 2.5 equiv of base; see Figures S2–S4). A linear correlation was found between variable base loadings and quenching as well (K_{SV} = 5,700 $\pm$ 500 M^{-1} and 4,800 $\pm$ 300 M^{-1} for amides and carbamates, respectively; see Figures S5–S11).[47]

The differences in quenching efficiency in these two experimental sets (with amide quenching being higher in the latter case) indicated that the base might have different affinity for amides versus carbamates. Hydrogen-bonding affinity constants were obtained via NMR titration (Figures 5 and S12–S15), with an amide affinity almost 45-fold higher than that of the carbamate (33 $\pm$ 4 M^{-1} for the amide and 0.74 $\pm$ 0.05 M^{-1} for the carbamate).[49] Interestingly, NMR titration showed a behavior close to saturation for the amide at loadings higher than 2.5 equiv, whereas for the carbamate, even upon addition of 5 equiv of base, no signs of saturation were observed. Expecting that near-saturation conditions would be ideal for a PCET mechanistic scenario, a reaction of carbamate **S43** with 7.5 equiv of $Bu_4N[OP(O)(OBu)_2]$ was carried out,[47] achieving a 14% yield increase within the same time frame (Figure 4, **43**). It is also noteworthy that, after adding *t*-BuOH to mimic the solvent system used in the reaction, a significant N–H chemical shift change from 7.19 to

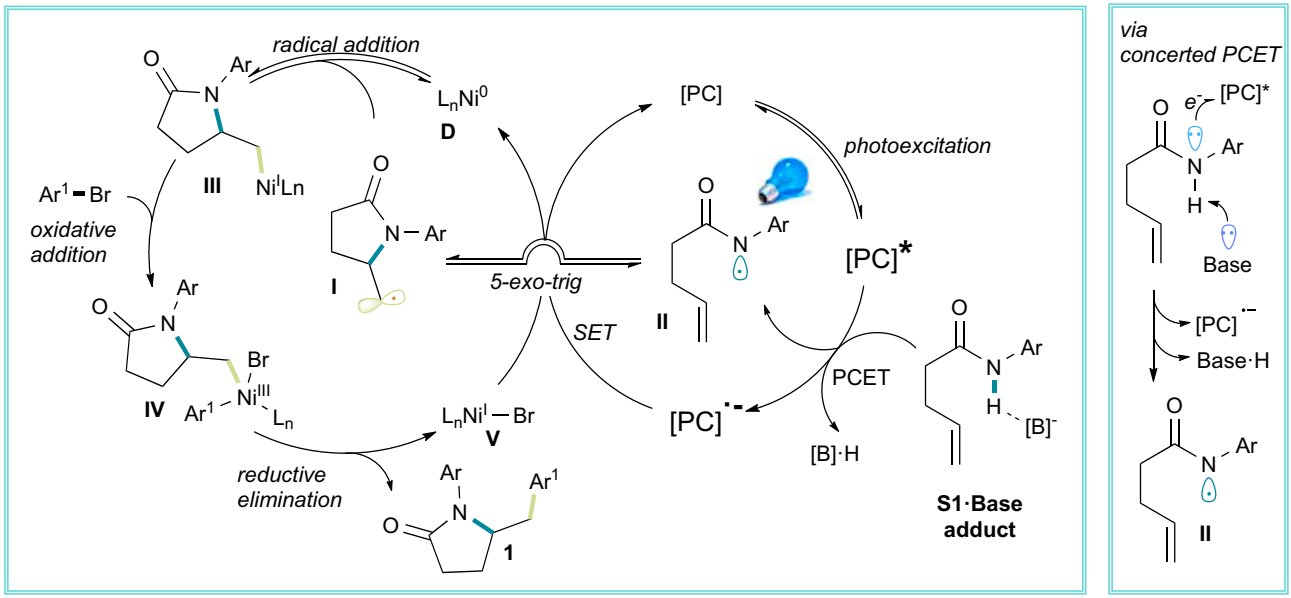

Scheme 3. Proposed Catalytic Cycle and PCET Mechanism

9.14 ppm was observed, which suggested a beneficial N–H acidity enhancement in the presence of *t*-BuOH (see Figure S16).[47] Under such reaction conditions, the substrate-base adduct would predominate and facilitate PCET, potentially via a proton wire-type mechanism.[50] Finally, kinetic isotope effects were measured with an *N*-deuterated amide and carbamate. Although both the amide and the carbamate revealed a small secondary kinetic isotope effect (KIE), the value for carbamate (1.08 ± 0.04) was still more significant than that for amide (1.02 ± 0.02) (see Scheme S1; Tables S2 and S3). Although small, KIEs are consistent with PCET processes,[14] and these data could indicate different rate-limiting steps between carbamates and amides. Further studies are required for a full understanding of such behavior.

Based on the previous empirical evidence gathered and precedent literature,[14,16,18,32,51] we propose a mechanistic scenario (Scheme 3) initiated by formation of an amidyl radical (**II**) via PCET as suggested by cyclic voltammetry, NMR experiments, and Stern-Volmer studies. Next, a fast 5-*exo-trig* cyclization follows, the rate of which is related to the nature of the newly formed alkyl radical and N–H BDE, as evidenced by indirect kinetic studies. Once the alkyl radical **I** is formed, it enters the nickel-catalytic cycle, forming Ni(I)-complex **III**, which undergoes oxidative addition with the aryl halide.[52] Next, the resultant high-valent Ni(III) intermediate **IV** undergoes reductive elimination, delivering the final product **1** along with a Ni(I)-halide complex (**V**). Both catalytic cycles are simultaneously closed by reduction of the Ni(I)-halide with the reduced form of the photocatalyst. Even though the key organonickel intermediates in the proposed mechanism proved challenging to isolate because of their highly reactive nature, their existence is in line with preliminary mechanistic investigations as well as previous computational studies on nickel/photoredox dual-catalyzed cross-coupling.[52]

Conclusion

A photoredox PCET/Ni dual-catalyzed amidoarylation of unactivated olefins has been disclosed, forging highly functionalized 5-membered heterocyclic systems under mild reaction conditions from readily available precursors. This method merges

the concept of concerted PCET with a nickel-catalyzed cross-coupling process for the first time, taking advantage of photocatalytic activation of strong N–H bonds assisted by a phosphate H-bond acceptor, followed by rapid 5-*exo*-*trig* cyclization and alkyl-aryl single-electron cross-coupling. Relative cyclization rates for amides and carbamates were studied, the latter being disclosed for the first time, which allowed the introduction of carbamates and ureas into the protocol. Stern-Volmer studies, NMR titration experiments, cyclic voltammetry, and control experiments point toward a concerted PCET mechanism. This transformation adds to the repertoire of alkene difunctionalization processes in a manner that is exceedingly functional group tolerant, using readily available alkenyl amides, carbamates, and ureas, and takes advantage of the tens of thousands of commercially available (hetero)aryl bromides and iodides to expand chemical space.

EXPERIMENTAL PROCEDURES

A general procedure for photoredox PCET/Ni-catalyzed amidoarylation of unactivated olefins is as follows. An 8.0-mL screw-cap vial containing a stirring bar was charged with Ni(dMeObpy) $(H_2O)_2(Br)_2$ (8.5 mg, 0.018 mmol, 6 mol %), $[Ir\{dF(CF_3)_2ppy\}_2(bpy)]PF_6$ (9.0 mg, 0.009 mmol, 3 mol %), amide (0.36 mmol, 1.2 equiv), aryl bromide (if solid, 0.3 mmol, 1.0 equiv), and $Bu_4N[(n\text{-}BuO)_2P(O)O]$ (338.8 mg, 0.75 mmol, 2.5 equiv). Next the vial was closed, and three vacuum/argon cycles were carried out. Under an inert atmosphere, a 2:1 mixture of pre-degassed, anhydrous *t*-BuOH/$PhCF_3$ was added (6.0 mL, 0.05 M) followed by addition of the aryl bromide (if liquid). After covering the cap with Parafilm, the reaction was placed 3 cm from the light source in a blue LED bay (blue LED strip, ~5 W in total) and stirred at room temperature until complete (a fan was added ~30 cm from above to disperse any heat coming from the blue LEDs). When completed, the reactions were taken to dryness and purified by column chromatography using an automated system (hexane/EtOAc gradient), delivering the corresponding pure product.

Other experimental details, characterization data (Figures S17–S177 and Tables S4–S39), and procedures are provided in Supplemental Information.

DATA AND SOFTWARE AVAILABILITY

Crystallographic data for the structures reported in this paper have been deposited at the Cambridge Crystallographic Data Center (CCDC), with accession numbers CCDC: 1854737 (Ni(dMeObpy) (H_2O) $(CH_3CN)_2Br_2$), 1854738 (**8**), 1854742 (**10**), 1854739 (**48**), 1854740 (**11**), and 1854741 (**9**).

SUPPLEMENTAL INFORMATION

Supplemental Information includes Supplemental Experimental Procedures, 177 figures, 1 scheme, 39 tables, and 6 data files and can be found with this article online at https://doi.org/10.1016/j.chempr.2018.11.014.

ACKNOWLEDGMENTS

The authors are grateful for the financial support provided by NIGMS (no. R01 GM 113878). We thank the NIH (no. S10 OD011980) for supporting the University of Pennsylvania (UPenn) Merck Center for High Throughput Experimentation, which funded the equipment used in screening efforts. Kai Chen (Caltech) is acknowledged for helpful discussion of the manuscript. The authors thank Dr. Jun Gu (UPenn) for assistance with the NMR studies, and Drs. P.J. Carroll and M.R. Gau (UPenn) for crystallographic analysis of compounds **8–11**, **48**, and the Ni-precatalyst.

AUTHOR CONTRIBUTIONS

A.G.-B. conceived the project; S.Z. and A.G.-B. designed the experiments; S.Z. and A.G.-B. carried out the experiments under the guidance of G.A.M.; S.Z. and A.G.-B. prepared the manuscript with input from G.A.M.

DECLARATION OF INTERESTS

The authors declare no competing interests.

Received: September 11, 2018
Revised: October 19, 2018
Accepted: November 20, 2018
Published: January 3, 2019

REFERENCES AND NOTES

1. Tellis, J.C., Primer, D.N., and Molander, G.A. (2014). Single-electron transmetalation in organoboron cross-coupling by photoredox/nickel dual catalysis. Science *345*, 433–436.

2. Zuo, Z., Ahneman, D.T., Chu, L., Terrett, J.A., Doyle, A.G., and MacMillan, D.W.C. (2014). Merging photoredox with nickel catalysis: coupling of α-carboxyl sp_3-carbons with aryl halides. Science *345*, 437–440.

3. Primer, D.N., Karakaya, I., Tellis, J.C., and Molander, G.A. (2015). Single-electron transmetalation: an enabling technology for secondary alkylboron cross-coupling. J. Am. Chem. Soc. *137*, 2195–2198.

4. Shields, B.J., and Doyle, A.G. (2016). Direct C(sp3)-H cross coupling enabled by catalytic generation of chlorine radicals. J. Am. Chem. Soc. *138*, 12719–12722.

5. Heitz, D.R., Tellis, J.C., and Molander, G.A. (2016). Photochemical nickel-catalyzed C-H arylation: synthetic scope and mechanistic investigations. J. Am. Chem. Soc. *138*, 12715–12718.

6. Tellis, J.C., Kelly, C.B., Primer, D.N., Jouffroy, M., Patel, N.R., and Molander, G.A. (2016). Single-electron transmetalation via photoredox/nickel dual catalysis: unlocking a new paradigm for sp3-sp2 cross-coupling. Acc. Chem. Res. *49*, 1429–1439.

7. Matsui, J.K., Lang, S.B., Heitz, D.R., and Molander, G.A. (2017). Photoredox-mediated routes to radicals: the value of catalytic radical generation in synthetic methods development. ACS. Catal. *7*, 2563–2575.

8. Johnston, C.P., Smith, R.T., Allmendinger, S., and MacMillan, D.W.C. (2016). Metallaphotoredox-catalysed sp3-sp3 cross-coupling of carboxylic acids with alkyl halides. Nature *536*, 322–325.

9. Lovering, F., Bikker, J., and Humblet, C. (2009). Escape from flatland: increasing saturation as an approach to improving clinical success. J. Med. Chem. *52*, 6752–6756.

10. However, there has been one exception recently, which required prefunctionalized imines and was merely restricted to dicyanophenyl derivatives Nakafuku, K.M., Fosu, S.C., and Nagib, D.A. (2018). Catalytic alkene difunctionalization via imidate radicals. J. Am. Chem. Soc. *140*, 11202–11205.

11. Vitaku, E., Smith, D.T., and Njardarson, J.T. (2014). Analysis of the structural diversity, substitution patterns, and frequency of nitrogen heterocycles among U.S. FDA approved pharmaceuticals. J. Med. Chem. *57*, 10257–10274.

12. The BDE of anilide N–H is ~99 kcal/mol. See Bordwell, F.G., Harrelson, J.A., and Lynch, T.Y. (1990). Homolytic bond dissociation energies for the cleavage of alpha-nitrogen-hydrogen bonds in carboxamides, sulfonamides, and their derivatives. The question of synergism in nitrogen-centered radicals. J. Org. Chem. *55*, 3337–3341.

13. Zhang, X.-M., and Bordwell, F.G. (1994). Acidities and homolytic bond dissociation enthalpies (BDEs) of the acidic H-A bonds in acyclic and cyclic alkoxycarbonyl compounds (esters and carbamates). J. Org. Chem. *59*, 6456–6458.

14. Choi, G.J., and Knowles, R.R. (2015). Catalytic alkene carboaminations enabled by oxidative proton-coupled electron transfer. J. Am. Chem. Soc. *137*, 9226–9229.

15. Nicolaou, K.C., Baran, P.S., Zhong, Y.L., and Sugita, K. (2002). Iodine(V) reagents in organic synthesis. Part 1. synthesis of polycyclic heterocycles via Dess-Martin periodinane-mediated cascade cyclization: generality, scope, and mechanism of the reaction. J. Am. Chem. Soc. *124*, 2212–2220.

16. Nicolaou, K.C., Baran, P.S., Zhong, Y.L., Barluenga, S., Hunt, K.W., Kranich, R., and Vega, J.A. (2002). Iodine(V) reagents in organic synthesis. part 3. new routes to heterocyclic compounds via o-iodoxybenzoic acid-mediated cyclizations: generality, scope, and mechanism. J. Am. Chem. Soc. *124*, 2233–2244.

17. Zhou, L., Tang, S., Qi, X., Lin, C., Liu, K., Liu, C., Lan, Y., and Lei, A. (2014). Transition-metal-assisted radical/radical cross-coupling: a new strategy to the oxidative C(sp3)-H/N-H cross-coupling. Org. Lett. *16*, 3404–3407.

18. Nicolaou, K.C., Baran, P.S., Kranich, R., Zhong, Y.-L., Sugita, K., and Zou, N. (2001). Mechanistic studies of periodinane-mediated reactions of anilides and related systems. Angew. Chem. Int. Ed. *40*, 202–206.

19. Chen, J.-R., Hu, X.-Q., Lu, L.-Q., and Xiao, W.-J. (2016). Visible light photoredox-controlled reactions of N-radicals and radical ions. Chem. Soc. Rev. *45*, 2044–2056.

20. Zard, S.Z. (2008). Recent progress in the generation and use of nitrogen-centred radicals. Chem. Soc. Rev. *37*, 1603–1618.

21. Kärkäs, M.D. (2017). Photochemical generation of nitrogen-centered amidyl, hydrazonyl, and imidyl radicals: methodology developments and catalytic applications. ACS. Catal. *7*, 4999–5022.

22. Wolff, M.E. (1963). Cyclization of N-halogenated amines (the Hofmann-Löffler reaction). Chem. Rev. *63*, 55–64.

23. Esker, J.L., and Newcomb, M. (1993). Amidyl radicals from *N*-(phenylthio)amides. Tetrahedron Lett. *34*, 6877–6880.

24. Esker, J.L., and Newcomb, M. (1993). Chemistry of amidyl radicals produced from N-hydroxypyridine-2-thione imidate esters. J. Org. Chem. *58*, 4933–4940.

25. Davies, J., Svejstrup, T.D., Fernandez Reina, D., Sheikh, N.S., and Leonori, D. (2016). Visible-light-mediated synthesis of amidyl radicals: transition-metal-free hydroamination and N-arylation reactions. J. Am. Chem. Soc. *138*, 8092–8095.

26. Fuentes, N., Kong, W., Fernández-Sánchez, L., Merino, E., and Nevado, C. (2015). Cyclization cascades via N-amidyl radicals toward highly functionalized heterocyclic scaffolds. J. Am. Chem. Soc. *137*, 964–973.

27. Miller, D.C., Choi, G.J., Orbe, H.S., and Knowles, R.R. (2015). Catalytic olefin hydroamidation enabled by proton-coupled electron transfer. J. Am. Chem. Soc. *137*, 13492–13495.

28. Choi, G.J., Zhu, Q., Miller, D.C., Gu, C.J., and Knowles, R.R. (2016). Catalytic alkylation of remote C-H bonds enabled by proton-coupled electron transfer. Nature *539*, 268–271.

29. Zhu, Q., Graff, D.E., and Knowles, R.R. (2018). Intermolecular anti-Markovnikov hydroamination of unactivated alkenes with sulfonamides enabled by proton-coupled electron transfer. J. Am. Chem. Soc. *140*, 741–747.

30. Warren, J.J., Tronic, T.A., and Mayer, J.M. (2010). Thermochemistry of proton-coupled electron transfer reagents and its implications. Chem. Rev. *110*, 6961–7001.

31. Weinberg, D.R., Gagliardi, C.J., Hull, J.F., Murphy, C.F., Kent, C.A., Westlake, B.C., Paul, A., Ess, D.H., McCafferty, D.G., and Meyer, T.G. (2012). Proton-coupled electron transfer. Chem. Rev. *112*, 4016–4093.

32. Chu, J.C.K., and Rovis, T. (2016). Amide-directed photoredox-catalysed C-C bond formation at unactivated sp3 C-H bonds. Nature *539*, 272–275.

33. Lan, X., Wang, N., and Xing, Y. (2017). Recent advances in radical difunctionalization of simple alkenes. Eur. J. Org. Chem. *39*, 5821–5851.

34. Liu, Z., Wang, Y., Wang, Z., Zeng, T., Liu, P., and Engle, K.M. (2017). Catalytic intermolecular carboamination of unactivated alkenes via directed aminopalladation. J. Am. Chem. Soc. *32*, 11261–11270.

35. Hanley, P.S., and Hartwig, J.F. (2013). Migratory insertion of alkenes into metal-oxygen and metal-nitrogen bonds. Angew. Chem. Int. Ed. *52*, 8510–8525.

36. Schultz, D.M., and Wolfe, J.P. (2012). Recent developments in Pd-catalyzed alkene aminoarylation reactions for the synthesis of nitrogen heterocycles. Synthesis *44*, 351–361.

37. Martinez, E., and Newcomb, M. (2006). Rate constants for anilidyl radical cyclization reactions. J. Org. Chem. *71*, 557–561.

38. Ney, J.E., and Wolfe, J.P. (2004). Palladium-catalyzed synthesis of *N*-aryl pyrrolidines from γ-(*N*-arylamino) alkenes: evidence for chemoselective alkene insertion into Pd-N bonds. Angew. Chem. Int. Ed. *43*, 3605–3608.

39. Yip, K.-T., and Yang, D. (2011). Pd(II)-catalyzed intramolecular amidoarylation of alkenes with molecular oxygen as sole oxidant. Org. Lett. *13*, 2134–2137.

40. Sahoo, B., Hopkinson, M.N., and Glorius, F. (2013). Combining gold and photoredox catalysis: visible light-mediated oxy- and aminoarylation of alkenes. J. Am. Chem. Soc. *135*, 5505–5508.

41. Fumagalli, G., Boyd, S., and Greaney, M.F. (2013). Oxyarylation and aminoarylation of styrenes using photoredox catalysis. Org. Lett. *15*, 4398–4401.

42. Trost, B.M., and Fandrick, D.R. (2003). Dynamic kinetic asymmetric cycloadditions of isocyanates to vinylaziridines. J. Am. Chem. Soc. *125*, 11836–11837.

43. Wu, C., Luo, X., Zhang, H., Liu, X., Ji, G., Liu, Z., and Liu, Z. (2017). Reductive amination/cyclization of levulinic acid to pyrrolidones versus pyrrolidines by switching the catalyst from $AlCl_3$ to $RuCl_3$ under mild conditions. Green. Chem. *19*, 3525–3529.

44. McMillen, D.F., and Golden, D.M. (1982). Hydrocarbon bond dissociation energies. Annu. Rev. Phys. Chem. *33*, 493–532.

45. Kumler, W.D., and Eiler, J.J. (1943). The acid strength of mono and diesters of phosphoric acid. the n-Alkyl esters from methyl to butyl, the esters of biological importance, and the natural guanidine phosphoric acids. J. Am. Chem. Soc. *65*, 2355–2361.

46. McNeece, A.J., Mokhtarzadeh, C.C., Moore, C.E., Rheingold, A.L., and Figueroa, J.S. (2016). Nickel bis-m-terphenylisocyanide dihalide complexes formed from 1,2-alkyl dihalides: probing for isolable β-haloalkyl complexes of square planar nickel. J. Coord. Chem. *69*, 2059–2068.

47. See Supporting Information for further details.

48. Wakchaure, V.N., Zhou, J., Hoffmann, S., and List, B. (2010). Catalytic asymmetric reductive amination of α-branched ketones. Angew. Chem. Int. Ed. *49*, 4612–4614.

49. Thordarson, P. (2011). Determining association constants from titration experiments in supramolecular chemistry. Chem. Soc. Rev. *40*, 1305–1323.

50. An effective way to translocate protons in biological system where a long-chain proton donor-acceptor complex is formed. For a reference, see Cárdenas, D.J., Cuerva, J.M., Alías, M., Buñuel, E., and Campaña, A.G. (2011). Water-based hydrogen-atom wires as mediators in long-range proton-coupled electron transfer in enzymes: a new twist on water reactivity. Chem. Eur. J. *17*, 8318–8323.

51. Musacchio, A.J., Nguyen, L.Q., Beard, G.H., and Knowles, R.R. (2014). Catalytic olefin hydroamination with aminium radical cations: a photoredox method for direct C-N bond formation. J. Am. Chem. Soc. *136*, 12217–12220.

52. Gutierrez, O., Tellis, J.C., Primer, D.N., Molander, G.A., and Kozlowski, M.C. (2015). Nickel-catalyzed cross-coupling of photoredox-generated radicals: uncovering a general manifold for stereoconvergence in nickel-catalyzed cross-couplings. J. Am. Chem. Soc. *137*, 4896–4899.